ASTRONOMY & ASTROPHYSICS
SUPPLEMENT SERIES

Astron. Astrophys. Suppl. Ser. **88,** 47-62 (1991)

Fibre spectroscopy and BV CCD photometry of the southern open cluster NGC 3114

Ram Sagar[1],[2],[3] and Ray M. Sharples[3],[4]

[1] Sternwarte der Universität Bonn, Auf dem Hügel 71, D-5300, Bonn 1, F.R.G.
[2] Indian Institute of Astrophysics, Bangalore 560034, India
[3] Anglo-Australian Observatory, P.O. Box 296, Epping, NSW 2121, Australia
[4] Department of Physics, University of Durham, South Road, Durham DH1 3LE, U.K.

Received August 16; accepted September 25, 1990

Abstract. — New spectroscopic and photometric observations are presented for a sample of faint stars which extends the colour-magnitude diagram of the open cluster NGC 3114 down to $V = 16$ mag. The distance to the cluster is estimated as 940 ± 60 pc. The spectroscopic observations indicate the presence of six CaII emitters in a sample of 55 stars. Radial velocity measurements and spectral classification have been carried out for all the 55 stars. Both spectroscopic and photometric observations indicate the presence of a large number of field stars in the direction of the cluster. Isochrones fitted to the colour-magnitude diagram as well as the position of the red giant concentration indicate that the age of the cluster is $\sim 1\text{-}2 \times 10^8$ yr.

Key words: star cluster: CCD photometry-fibre spectroscopy-radial velocity, emission lines.

1. Introduction.

The southern Galactic open cluster NGC 3114 (C1001-598; $l = 283°.34$, $b = 3°.83$) is located in a fairly rich Milky way field in Carina and has been classified as Trumpler class II3r (Lyngå, 1987). Although the cluster is rich, its members are difficult to study because of the heavy contamination from field stars. Photometric observations have been made for stars brighter than $V \sim 12.5$ by Lyngå (1962), Jankowitz and McCosh (1963, hereafter JM), Schmidt (1982) and more recently by Schneider and Weiss (1988). The presence of a large number of background B stars in the field, fainter than $B = 11.2$ mag, has been demonstrated by Lyngå (1962) on the basis of the evolutionary deviation curve of the cluster. Using Strömgren photometry of bright B- and A- type cluster members, Schneider and Weiss (1988) found $E(B-V) = 0.03$ mag for the cluster reddening which is in good agreement with the value of 0.04 mag found earlier by Lyngå (1962) and Schmidt (1982) but is smaller than the value 0.09 mag given by JM. Other cluster parameters taken from the catalogue of Lyngå (1987) are a distance $D = 900$ pc, an age $\tau = 10^8$ yr and a mean metallicity of [Fe/H] =0.01. Spectroscopic studies (Frye *et al.*, 1970; Levato and Malaroda, 1975; Harris, 1976; Henize, 1976) of stars brighter than $V \simeq 12$ mag indicate the presence of a significant number of peculiar stars in the cluster. Based on the radial velocity measurements of 169 stars, Amieux and Burnage (1981) indicate that the cluster has a mean radial velocity of 2.5 km s^{-1} and an angular diameter of more than 52 arcmin. Astrometric positions with an accuracy of 0.1 arcsec for 260 stars in the cluster field have been given by Andersen and Reiz (1983, hereafter AR).

In this paper we describe new spectroscopic observations of a sample of faint ($V \sim 14$ mag) stars in the field of NGC 3114 obtained using a fibre-coupled multi-object spectrograph. We also present new BV CCD photometry which extends the colour-magnitude diagram (CMD) of the cluster to $V = 16$ mag and enables a more accurate estimate of the cluster distance to be made.

2. Observations.

The spectroscopic and photometric observations were made independently and are described in the following subsections.

2.1. SPECTROSCOPY.

The spectroscopic observations were obtained during commissioning runs of a new automatic fibre positioner (Autofib) at the 3.9 m Anglo-Australian Telescope (AAT) in March 1987. Briefly, this device uses a robot positioner to place rapidly up to 64 magnetically located fibre probes at

the positions of target objects within a field of 40 arcmin diameter. The output of the fibre bundle is then fed to a conventional long-slit spectrograph. Full details of the instrument can be found in Parry and Gay (1986) and Parry and Sharples (1988).

In order to test the positioning accuracy of Autofib, we selected a sample of 55 stars in NGC 3114 with accurate (0.1 arcsec) co-ordinates given by AR. The remaining fibres were dedicated to monitor the sky background across the field which was particularly bright due to the presence of a nearly full Moon. During the observations, the telescope was raster scanned around the nominal field centre in two 5 x 5 grid with spacing of 0.5 and 1.0 arcsec respectively. Integration times at each grid position were 150 sec. By analysing the distribution of count rates around the grids, the positioning accuracy of each fibre probe could be derived and was found to be $\sim$ 0.3 arcsec. By summing the data at all positions in the rasters, a mean spectrum for each star was obtained which, although of somewhat poorer quality than would be achieved during normal observations, gave useful spectral information for stars in a region of the CMD not previously studied in this cluster.

The fibres were fed to the RGO spectrograph in which a 25 cm camera and a 1200 line grating blazed at 4000 Å were employed; the detector used was the Image Photon Counting System (IPCS). The spectra cover the wavelength range 3750-4650 Å at a reciprocal dispersion of 33 Å/mm and a pixel size of 1 Å. The 300 μ (2.0 arcsec) fibres used gave a spectral resolution of 2 Å.

2.2. PHOTOMETRY.

Since the limiting magnitude for available photometric observations is $V \sim 13$ mag, most of the stars studied spectroscopically do not have photometric measurements. In order to derive their magnitudes, we have used a short (5 minute exposure) prime focus photographic plate taken at the AAT using IIaO emulsion and a GG385 filter. This plate was scanned with a PDS microdensitometer using small rasters of 25 x 25 arcsec^2 with a step size of 0.5 arcsec centered on the position of each spectroscopic star. Two larger regions of 5 x 4 arcmin^2 were also scanned at the same time for calibration purposes (see Sect. 3.1.2).

To calibrate the photographic magnitudes and determine the form of the CMD at fainter magnitudes, seven regions centered around a subsample of the spectroscopic stars (see Fig. 1) were imaged in the B and V photometric passbands using a CCD. The observations were made between 22 - 28 June 1989 using a dye-coated GEC P8603 device (578 x 385 pixel^2) at the f/8 cassegrain focus of the ANU 1.0 m telescope located at Siding Spring Observatory. Each pixel on the CCD corresponds to 0.56 arcsec on the sky. The read out noise for the system was about 7 electrons per pixel. Exposures ranging from 1 to 90 seconds were taken for programme stars; flat field exposures were made using the twilight sky. As these observations were carried out during another main observing programme, further details of the instrument and observing procedure have been described there (Sagar and Cannon, 1991).

3. Data reduction.

Details of the photometric and spectroscopic data reductions are given below.

3.1. PHOTOMETRIC REDUCTIONS.

The photometric reductions can be divided into two groups, the CCD photometry and the photographic photometry.

3.1.1. *CCD photometry.*

Bias substraction and flat-field corrections to the CCD photometry were applied using the FIGARO data reduction package on the Epping VAX 11/780 and μ VAX 3500 computers at the Anglo-Australian Observatory. The uniformity of the flat-fields is better than a few percent in both filters. Although the field is not exceptionally crowded, the magnitude estimates have been obtained using the DAOPHOT profile-fitting software (Stetson, 1987) in order that the CMD can be determined reliably to faint levels. In some filters we have more than one CCD frame of a region. In such cases, the magnitudes were averaged and have been used in the further discussions.

Zero-points for each region have been estimated from E-region standards (Graham, 1982); these cover a range in brightness (12.3 mag $\leq V \leq$ 16.5 mag) as well as colour (0.06 mag $\leq (B-V) \leq$ 1.61 mag). In evaluating the zero-points, we have simply taken into account the difference in exposure times and used mean atmospheric extinction coefficients. We have used the colour equations given by Sagar and Cannon (1991), as the present observations were carried out during the same period. The zero-points have an uncertainty of $\sim$ 0.04 mag in B and V. The internal errors estimated from the scatter in the individual measures on different frames are listed in Table 1 as a function of V magnitude.

TABLE 1. *Internal photometric errors of CCD observations as a function of brightness; σ is the standard deviation per observation in magnitudes.*

Magnitude range	σ_B	σ_V
$\leq$ 13.0	0.017	0.012
13.0 – 14.0	0.022	0.018
14.0 – 15.0	0.028	0.022
15.0 – 16.0	0.035	0.032

The relative α and δ positions in arcsec with respect to $\alpha_{1950} = 10^h02^m$; $\delta_{1950} = -60°00'$ as well as V and $(B-V)$ magnitudes of the stars are listed in Table 2. The number of observations in the V and B filters are denoted by N_v and N_b respectively. Stars observed by Lyngå (1962), JM and AR have been prefixed with L, JM and AR in the *last column*. The relative positions have been obtained by transforming the X and Y pixel coordinates of the stars using the astrometric positions given by AR to define a local reference frame on each CCD image.

As a check on the accuracy of our independently determined zero points, we have compared the present photometry with photoelectric determinations by Lyngå (1962) and JM which agree well with each other (cf. Schneider and Weiss, 1988). Although this comparison is possible only for the six brighter stars, namely JM127, 154, 182, 196, 211 and 212 (cf. Mermilliod, 1986), the agreement is generally excellent and confirms the estimate above for the precision of the zero-points. The largest residuals are for stars JM127 and 212 ($|\Delta V| = 0.13$ and 0.11 mag respectively), and in both cases the CCD magnitudes, determined form the profile-fitting technique, are fainter than the photoelectric ones. Inspection of their images on the CCD frames reveals that they have 3-4 faint stellar companions. The agreement becomes much better if the total light from the stars and their companions is compared with the photoelectric measurements. This indicates that the errors are more likely to lie in the photoelectric observations which have been carried out using an aperture which probably included the fainter stellar companions.

3.1.2. *Photographic photometry.*

Photographic photometry of the spectroscopic stars was obtained using an aperture magnitude routine to integrate the density within a 15 arcsec aperture centered on each star. In order to calibrate these values, we have also derived aperture magnitudes for all stars in the range *B=12-16 mag* in two of the CCD fields (R3 and R7) shown in Figure 1. Figure 2 shows the relation between these photographic magnitudes and the CCD magnitudes from Table 2 for stars in common; the calibration has been fitted by a second order polynomial with rms residuals ~ 0.18 mag and there is no indication of any systematic offset between the two fields. This mean relation was therefore used to transform the photographic data for all the spectroscopic stars onto the CCD system, with the results listed in Table 4. Comparisons of the transformed data are shown in Table 3 and Figure 3 for the 12 spectroscopic stars with independent CCD photometry and another 5 with photoelectric or photographic photometry from JM.

3.2. SPECTROSCOPIC REDUCTIONS.

The spectra were extracted from the 2-dimensional IPCS frames by fitting polynomials to the position of each fibre spectrum, which is curved due to S-distortion in the magnetically focussed image tube. The wavelength distortion was then mapped using exposures of a hollow cathode CuAr lamp and the data rebinned to a linear wavelength scale with errors of < 0.3 Å. Because of vignetting within the spectrograph and small angular misalignments at the entrance apertures of the fibres, the transmission of the system varies from fibre to fibre. Tests of the stability of the throughput, however, indicate that this variation is very stable and can be adequately corrected using an exposure of the twilight sky. Sky subtraction was therefore performed using the mean spectrum from the 9 dedicated sky fibres. A few representative spectra are shown in Figure 4. Details of the derivation of line and continuum indices, spectral classification and radial velocity measurements from these spectra are given below.

3.2.1. *Radial velocity measurements.*

Radial velocities for the programme stars were derived using a standard cross correlation technique (e.g. Tonry and Davis, 1979). As no radial velocity templates were observed during the commissioning runs, we have used representative stars from the library of stellar spectra published by Jacoby *et al.* (1984) which have a similar resolution and spectral coverage. To ensure a good match to the range of spectra in the programme stars (see Fig. 4) we have cross-correlated each star with three templates: HD111525 (A7V), HD23511 (F4V) and HD33278 (G9V) and adopted the relative velocity given by the cross-correlation function with the highest peak value. Relative velocities of the three templates could be determined to an accuracy ~ 3 km s^{-1} using programme stars of intermediate spectral types. Finally the velocities have been reduced to a heliocentric system by measuring the wavelengths of the Hγ, Hδ and CaII (λ3933 Å) lines in a sample of 10 late-F stars in the cluster sample which had good S/N (and in which these lines are particularly strong). Effective wavelengths for these lines were taken from the compilation of Shawl *et al.* (1985). The uncertainty of the absolute velocity zero point is estimated to be ± 30 km s^{-1}. Heliocentric velocities and internal errors (excluding the possible zero-point error) are given in Table 4.

3.2.2. *Spectral classification and (B-V) colour*

In order to derive $B-V$ colours for the stars in spectroscopic sample, we have used a technique of spectral classification based on the cross-correlation method. Each star was first cross-correlated with all 161 of the stellar templates in the Jacoby *et al.* (1984) atlas of spectral energy distributions, after rebinning the latter to the same wavelength range and resolution as the present data. The distribution of R-values of the correlation function (the ratio of peak height to rms noise - see Tonry and Davis, 1979) was then examined. The best match (defined as that giving the highest R-value) for luminosity class III to V stars was selected and the synthe-

sised (dereddened) colours taken from Table 2 of Jacoby *et al.* (1984). None of our sample are expected to be luminosity class I or II stars since an early-type supergiant with $V \sim 14$ would have $D > 150$ kpc. Our adopted colours and spectral types are listed in *columns 3 and 4* of Table 4. Note that this classification is essentially based on relative line strengths since the continuum shape is removed by fitting a low-order polynomial prior to the cross-correlation stage. At this resolution and S/N the subtle luminosity-sensitive lines are difficult to measure reliably and in many cases the difference in R-values between templates of different luminosity-class (but the same spectral type) is small and possibly affected by noise in the spectra. We therefore caution that the luminosity class listed in Table 4 is reliable only for a few cases (mostly of later spectral types) where differences in the peak heights become significant. A comparison of the spectroscopically determined colours with those from CCD, photoelectric and photographic photometry (cf Sect. 3.1.2.) is given in Table 3 and plotted in Figure 3.

3.2.3. *Line indices and continuum ratios.*

In order to search for CaII H and K emission line stars in the cluster, we have used the line indices and continuum ratios defined by Collier Cameron and Reid (1987) in their study of chromospheric emission lines in open clusters:

$$(3912/3990) = \sum_{3905}^{3920} F_\lambda / \sum_{3980}^{4000} F_\lambda$$

$$H = \sum_{3923}^{3943} F_\lambda / \left(\sum_{3905}^{3920} F_\lambda + \sum_{3980}^{4000} \right) F_\lambda$$

$$K = \sum_{3958}^{3978} F_\lambda / \left(\sum_{3905}^{3920} F_\lambda + \sum_{3980}^{4000} \right) F_\lambda$$

$$Ca = H + K$$

$$HK = \frac{\sum_{3931}^{3935} F_\lambda + \sum_{3966}^{3970} F_\lambda}{\sum_{3925}^{3975} F_\lambda - \sum_{3931}^{3935} F_\lambda - \sum_{3966}^{3970} F_\lambda}$$

where F_λ is the photon flux in rest wavelength bin λ. Line indices and errors (calculated from photon statistics) are listed in Table 5 for each of the programme stars and plotted in Figure 5. The excellent correlation observed in these Figures indicates that the indices are accurately measuring line strengths and are not seriously affected by uncertainties in sky-subtraction, wavelength calibration etc.

Collier Cameron and Reid (1987) note that the HK index is the most sensitive indicator of CaII H and K emission and we have therefore plotted this index against $(B-V)$ in Figure 6. For all except 6 of the programme stars (AR17, 78, 95, 121, 144 and 222) the value of HK index is < 0.1. Of the remaining 49 stars, those with redder colours ($(B-V) > 0.9$ mag) have a slightly lower mean HK index (0.06 ± 0.01) than that for the blue stars (0.08 ± 0.01). Collier Cameron and Reid (1987) have shown that the presence of emission lines in the CaII H and K line cores comparable to those exihibited by typical RS CVn binaries in the solar neighbourhood, will increase the HK index by between 0.03 and 0.2. Given that the rms errors in our indices are typically ± 0.007, the value of the HK index for the 6 stars with $HK > 0.1$ lies $> 3\sigma$ above the mean locus. We have therefore labelled them as CaII emitters in Table 5. In the next section, we show that all have been classified as main-sequence stars with spectral types between A6 and F8. Their status as cluster members is discussed in section 6.

4. Colour-magnitude diagram and field star contamination.

In Figure 7, we have plotted V, $(B-V)$ CMD of all the stars listed in Table 2. Most of them are fainter than $V \sim 12$ mag and hence, the cluster sequence towards the brighter part of the CMD can not be seen. For this magnitude range, we have plotted stars which have photoelectric BV data in the catalogue of Mermilliod (1986). Those spectroscopic stars which do not have either CCD or photoelectric measurements have been plotted as filled circles in Figure 7 using data from Table 4. In the magnitude range $V = 9 - 13$ mag, the cluster sequence formed by the photoelectric data merges smoothly with that formed by the present CCD observations. This further strengthens the reliability of the zero point estimates for the CCD data.

A well defined cluster main sequence is clearly visible in the magnitude range $V = 7 - 13$ mag. A group of stars located in a region of the CMD defined by $7.0 < V < 9.5$ and $0.9 < (B-V) < 1.3$ probably form the red giant tip of the cluster sequence. A large amount of scatter is present in those stars fainter than $V \sim 13.5$ mag. This cannot be due to random errors present in our observations (cf. Tab. 1), and most likely results from the presence of a large number of background and foreground stars in the sample. The presence of such stars in the brighter part of the CMD has already been indicated by Lyngå (1962). Clearly the luminosity function of the cluster does not rise steeply enough to dominate the field star contribution at fainter magnitudes.

5. Distance to the cluster.

The distance to NGC 3114 has been estimated by fitting the zero-age main-sequence (ZAMS) given by Schmidt-Kaler (1982) to the data in Figure 7 over the magnitude range $V = 11 - 14$ mag. Brighter stars are likely to have been affected by evolutionary changes (see Sect. 7) and fainter than this limit, the cluster main-sequence is badly contaminated by field stars. For this calculation, a value of $E(B-V) = 0.04$ mag, as indicated by recent observations (cf. Sect. 1),

has been used for the reddening to the cluster. The best-fit ZAMS, shown in Figure 7, corresponds to an apparent distance modulus, $(m-M) = 10.0 \pm 0.2$ mag. Using the above value of $E(B-V)$ and a value of 3.15 for the ratio of total to selective absorption, we derive a distance of 940 ± 60 pc to the cluster. This value is in excellent agreement with that given in the catalogue of Lyngå (1987).

6. Membership of the spectroscopic stars.

In order to decide the cluster membership of stars observed spectroscopically, we have used both photometric and spectroscopic data obtained in Sect. 3. A histogram of the radial velocity data is shown in Figure 8. There is no clear cut separation of cluster members from field stars. This is because the mean heliocentric radial velocity of the cluster is ~ 2.5 km s^{-1} (cf. Sect. 1) which is not too different from the radial velocity expected for Galactic disk stars in this direction (Amieux and Burnage, 1981). However, the possibility of cluster membership is small for the 18 stars with radial velocity either < -20 km s^{-1} or > 25 km s^{-1}. Cluster membership of the remaining stars has been decided on the basis of their distance modulus estimated from the spectral classification and the photometry given in Table 4. For this, we have used the relation between M_v and spectral class given by Schmidt-Kaler (1982). Allowing for the effects of binarity and errors in the photographic and spectroscopic measurements, we have considered stars with $(m - M_v) = 10.0 \pm 1.5$ to be probable cluster members. Because of the difficulty of determining luminosity classes from the spectroscopic data alone (cf. Sect. 3.2.2) we have also applied the constraint that probable cluster members must lie within ± 0.25 mag of the ZAMS in Figure 7. With these criteria, only 13 stars out the sample of 55 are likely to be cluster members (denoted by *M* in *column* 7 of Table 4). Clearly this analysis indicates the presence of a large number of field stars in the direction of the cluster and supports the conclusion of section 4. A detailed investigation of the cluster membership at faint magnitudes will, however, require the use of more accurate methods such as proper motion studies.

Amongst the possible CaII emitters discussed in section 3.2.3, only 3 (AR17, 78 and 95) are probable cluster members. However, this fraction is still somewhat higher than that found by Collier Cameron and Reid (1987) in their survey of the old (3–7 Gyr) open clusters NGC 2204, 2243, 2420, 2506 and Melotte 66.

7. Cluster age.

The age of NGC 3114 has been estimated by fitting theoretical and empirical isochrones to the CMD and also by using the location of the red giant concentration in Figure 7. The revised Yale isochrones for $Z = 0.01$, $Y = 0.20$ and $\tau = 150$ and 350 Myr (Green *et al.*, 1987) and empirical isochrones for the Pleiades, NGC 2516, 2287 and 6475 age groups given by Mermilliod (1981) have been fitted to the CMD of the cluster in Figure 9a and 9b respectively. The best-fit isochrone in both diagrams indicates that cluster is $\sim 2 \times 10^8$ yrs old.

The mean absolute magnitude of the red giant concentration is found to be at $M_v = -1.9$ mag. Based on the relation between M_v and cluster age given by Mermilliod (1981), this value of M_v yields $\log \tau = 8.1$ for the cluster NGC 3114. Therefore, we conclude that age of the cluster is $1 - 2 \times 10^8$ yrs, which is in good agreement with the value of $\log \tau = 8.03$ given in the catalogue of Lyngå (1987).

8. Conclusions.

We have presented fibre spectroscopic and BV CCD photometric data for a sample of 55 and 358 stars respectively in the region of the young open cluster NGC 3114. Radial velocities, spectral classifications and spectral line indices have been estimated for all the stars observed spectroscopically. The HK index indicates the presence of CaII H and K line emission in six stars, of which 3 are probable cluster members. A distance of 940 ± 60 pc has been estimated to the cluster by fitting thr ZAMS in the CMD. Both spectroscopic and photometric observations indicate the presence of a large number of faint ($V \geq 13.5$ mag) field stars in the direction of NGC 3114. Isochrone fits to the CMD and the mean absolute magnitude of the red giant concentration both indicate an age of $1 - 2 \times 10^8$ yrs.

Acknowledgements.

We gratefully acknowledge the Anglo-Australian Observatory and Mount Stromlo and Siding Spring Observatories for the allotment of telescope time for this project. We are grateful to Barry Croke, Peter Gray, William Lupton and Ian Parry for providing assistance during observations and reductions. One of us (RS) gratefully acknowledge the Department of Industry, Technology and Commerce of Australia, the IAU, and the Alexander von Humboldt Foundation for providing financial support.

References

Amieux G. and Burnage R.: 1981, *Astron. Astrophys. Suppl. Ser.* **44**, 101.
Andersen T.B. and Reiz A.: 1983, *Astron. Astrophys. Suppl. Ser.* **53**, 181.
Collier Cameron A. and Reid N.: 1987, *Mon. Not. R. Astron. Soc.* **224**, 821.
Frye R.L., Mac Connell D.J. and Humphreys R.M.: 1970, *Publ. Astron. Soc. Pac.* **82**, 1360.
Green E.M., Demarque P. and King C.R.: 1987, In: The Revised Yales Isochrones and Luminosity Functions, Yale University Observatory (New Haven USA).
Graham J.A.: 1982, *Publ. Astron. Soc. Pac.* **94**, 244.
Harris G.L.H.: 1976, *Astrophys. J. Suppl. Ser.* **30**, 451.
Henize K.G.: 1976, *Astrophys. J. Suppl. Ser.* **30**, 491.
Jacoby G.H., Hunter D.A. and Christian C.A.: 1984, *Astrophys. J. Suppl. Ser.* **56**, 257.
Jankowitz N.E. and McCosh C.J.: 1963, *Mon. Not. Astron. Soc. S. Afr.* **22**, 18.
Levato H. and Malaroda S.: 1975, *Astron. J.* **80**, 807.
Lyngå G.: 1962, *Ark. Astron.* **3**, 65.
Lyngå G.: 1987, Catalogue of Open Cluster Data, 5th edition, 1/1 S7041, Centre de Donnees Stellaires (Strasbourg).
Mermilliod J.-C.: 1981, *Astron. Astrophys.* **97**, 235.
Mermilliod J.-C.: 1986, *Bull. Inform. CDS* No 31, 175.
Parry I.R. and Gray P.M.: 1986, *Proceedings of S.P.I.E.* **627**, 303.
Parry I.R. and Sharples R.M.: 1988, Astronom. Soc. Pacif. Conference Series, Vol. 3, ed. S.C. Barden, p. 63.
Sagar R. and Cannon R.D.: 1991, in preparation.
Schmidt E.G.: 1982, *Publ. Astron. Soc. Pac.* **94**, 232.
Schmidt-Kaler Th.: 1982, Landolt/Bornstein, Numerical Data and Functional Relationship in Science and Technology, New Series, Group VI, Vol. 2(b), K. Schaifers and H.H. Voigt Eds. (Springer-Verlag, Berlin) p. 14.
Schneider H. and Weiss W.W.: 1988, *Astron. Astrophys. Suppl. Ser.* **75**, 353.
Shawl S.J., Hesser J.E., Meyer J.E. and van Heteren J.: 1985, *Publ. Astron. Soc. Pac.* **97**, 519.
Stetson P.B.: 1987, *Publ. Astron. Soc. Pac.* **99**, 191.
Tonry J. and Davis M.: 1979, *Astron. J.* **84**, 1511.

TABLE 2. *Positions and magnitudes of stars with CCD photometry in NGC 3114.*

Star	$\Delta\alpha$ (arcsec)	$\Delta\delta$ (arcsec)	V (mag)	(B-V) (mag)	N_v	N_b	Other Identifications
Region 1							
1	-891.4	-604.6	13.89	0.45	1	1	
2	-893.4	-660.9	15.49	0.51	1	1	
3	-913.6	-661.3	14.33	0.98	1	1	
4	-924.7	-599.2	14.85	0.92	1	1	
5	-935.0	-535.4	15.78	1.05	1	1	
6	-942.9	-671.1	15.25	1.22	1	1	
7	-997.0	-571.0	14.90	1.15	1	1	
8	-1004.7	-574.5	15.89	0.80	1	1	
9	-1037.2	-701.2	14.30	0.55	1	1	
10	-1045.1	-690.6	15.37	0.48	1	1	
11	-1073.6	-719.9	12.91	0.54	1	1	
12	-1076.4	-628.6	14.43	1.06	1	1	
13	-1089.8	-539.4	15.48	0.70	1	1	
14	-1121.2	-590.1	13.70	0.67	1	1	
15	-1165.7	-704.4	15.88	0.61	1	1	
16	-1186.4	-718.6	15.15	0.67	1	1	
17	-1201.9	-537.1	15.40	1.36	1	1	
18	-1206.7	-598.5	13.52	0.44	1	1	AR95
19	-1225.2	-632.6	13.78	0.32	1	1	
20	-1227.1	-720.2	15.23	1.66	1	1	
21	-1247.7	-602.8	14.12	1.27	1	1	
22	-1252.6	-579.7	15.42	0.58	1	1	
23	-1256.2	-640.0	14.84	0.73	1	1	
24	-1255.8	-584.9	14.22	1.08	1	1	
25	-1257.1	-637.2	14.25	0.54	1	1	
26	-1258.9	-666.9	14.11	0.53	1	1	
27	-1261.2	-601.1	14.78	0.80	1	1	
28	-1264.8	-522.5	14.75	0.99	1	1	
29	-1279.1	-661.2	13.34	0.65	1	1	
30	-1281.6	-672.7	15.84	0.51	1	1	
31	-1293.8	-541.8	15.41	0.48	1	1	
32	-1298.9	-710.1	13.49	0.42	1	1	AR92
33	-1317.1	-601.2	15.72	0.57	1	1	
34	-1318.1	-592.4	15.62	0.54	1	1	
35	-1336.3	-712.5	15.77	1.08	1	1	
36	-1340.8	-634.2	14.21	0.72	1	1	
37	-1348.2	-547.4	15.52	1.34	1	1	
38	-1366.0	-593.0	14.65	0.82	1	1	
39	-1403.7	-622.6	15.81	0.44	1	1	
40	-1404.8	-661.8	15.88	0.40	1	1	
41	-1408.1	-537.5	14.55	1.14	1	1	
42	-1409.9	-696.2	14.66	1.19	1	1	
43	-1409.5	-630.0	14.23	0.28	1	1	
44	-1409.9	-600.5	15.15	0.66	1	1	
45	-1420.3	-673.8	15.87	0.49	1	1	
46	-1471.3	-697.0	15.95	0.55	1	1	
47	-1482.8	-624.6	15.70	0.55	1	1	
48	-1499.5	-669.2	13.84	0.52	1	1	
49	-1501.2	-675.7	14.24	0.59	1	1	
50	-1510.9	-543.7	14.60	0.70	1	1	
Region 2							
1	-58.4	-302.2	14.92	0.51	1	1	
2	-73.2	-333.1	14.52	0.14	1	1	AR160
3	-90.9	-289.1	14.17	0.33	1	1	
4	-96.8	-203.4	15.77	0.60	1	1	
5	-130.3	-358.4	14.07	1.01	1	1	
6	-132.6	-280.3	15.74	0.42	1	1	
7	-133.5	-366.7	13.70	0.73	1	1	
8	-157.5	-223.9	14.48	0.50	1	1	
9	-181.7	-233.9	15.11	1.18	1	1	
10	-188.9	-398.8	15.96	0.88	1	1	
11	-194.2	-234.9	14.97	1.81	1	1	
12	-197.6	-321.2	15.56	0.60	1	1	
13	-199.6	-282.7	14.48	1.44	1	1	
14	-233.3	-230.3	15.55	1.28	1	1	
15	-245.8	-280.9	11.84	0.09	1	1	JM154
16	-254.7	-255.2	15.96	0.71	1	1	
17	-257.9	-283.9	14.35	0.51	1	1	
18	-272.3	-270.7	12.04	0.12	1	1	
19	-277.3	-229.8	12.03	1.40	1	1	
20	-307.7	-340.5	15.51	0.49	1	1	
21	-307.1	-228.9	15.79	1.15	1	1	
22	-324.7	-367.3	14.13	0.27	1	1	AR144
23	-349.1	-238.1	14.45	0.63	1	1	
24	-367.6	-234.3	15.81	0.50	1	1	
25	-376.4	-247.8	13.96	1.40	1	1	
26	-385.7	-222.1	15.48	0.72	1	1	
27	-401.5	-361.9	15.86	0.59	1	1	
28	-418.8	-384.8	14.21	0.34	1	1	
29	-423.9	-231.4	15.50	0.64	1	1	
30	-446.2	-346.3	14.10	1.05	1	1	
31	-451.8	-300.3	15.54	0.57	1	1	
32	-459.3	-366.9	15.53	0.67	1	1	
33	-470.6	-371.9	13.57	1.18	1	1	
34	-485.2	-374.6	14.45	0.64	1	1	
35	-488.8	-375.1	13.86	1.45	1	1	
36	-490.9	-298.0	15.03	1.32	1	1	
37	-500.0	-328.2	15.97	0.62	1	1	
38	-507.3	-368.5	13.10	1.38	1	1	
39	-510.0	-240.8	15.67	1.15	1	1	
40	-512.2	-278.1	15.49	0.44	1	1	
41	-515.7	-313.9	14.73	0.57	1	1	
42	-522.2	-314.5	11.31	0.94	1	1	JM127,L23
43	-530.3	-378.4	15.44	0.52	1	1	
44	-542.9	-332.3	15.68	0.48	1	1	
45	-545.9	-368.9	14.15	0.38	1	1	
46	-554.8	-324.9	15.18	0.68	1	1	
47	-571.1	-395.5	13.26	0.22	1	1	
48	-576.4	-349.0	14.75	0.54	1	1	
49	-591.9	-300.2	15.20	0.53	1	1	
50	-593.7	-315.4	14.29	0.55	1	1	
51	-629.1	-246.8	14.92	0.57	1	1	
52	-632.6	-206.4	15.74	1.16	1	1	
53	-691.5	-263.9	13.67	0.51	1	1	AR124
Region 3							
1	520.4	1177.9	13.40	1.64	4	4	
2	467.8	1233.6	13.19	0.36	4	4	AR199
3	467.2	1300.2	9.57	-0.11	4	4	JM196,L15
4	461.3	1249.3	14.68	1.23	4	4	
5	459.2	1151.1	14.99	1.64	4	3	
6	446.8	1195.0	15.46	1.26	4	4	
7	427.0	1315.2	15.01	0.66	4	4	
8	353.2	1188.6	14.49	1.32	4	4	
9	352.3	1250.7	15.38	1.18	4	4	
10	346.8	1229.1	13.51	0.58	4	4	AR194
11	334.8	1302.3	14.39	1.23	4	4	
12	329.1	1174.4	15.74	0.61	4	3	
13	290.8	1318.9	15.63	0.62	4	4	
14	288.3	1180.8	14.48	0.44	4	4	
15	274.8	1321.9	15.49	0.46	4	4	
16	267.8	1275.6	14.88	1.31	4	4	
17	221.1	1160.2	11.63	0.05	4	4	JM182,L25
18	209.2	1231.8	15.84	0.62	4	4	
19	199.6	1287.1	14.54	0.24	4	4	
20	168.9	1150.0	15.43	0.71	4	3	
21	145.5	1197.9	15.75	0.72	4	4	
22	145.3	1164.6	15.33	0.67	4	4	
23	129.0	1161.9	15.29	0.89	4	4	
24	121.1	1238.7	14.10	1.21	4	4	
25	77.6	1201.7	15.94	0.51	4	4	
26	44.5	1232.1	14.08	0.49	4	4	AR169
27	39.3	1288.3	13.06	1.18	4	4	AR167
28	38.7	1142.6	14.07	0.63	4	3	
29	38.4	1144.3	14.73	0.51	4	3	
30	25.2	1181.2	14.63	0.38	4	4	
31	14.5	1235.5	14.66	0.55	4	4	
32	5.3	1317.3	11.30	0.94	4	4	
33	-3.1	1169.1	14.49	0.55	4	4	
34	-4.6	1123.3	15.66	1.27	4	2	
35	-13.6	1325.0	15.99	0.77	4	2	

TABLE 2. *(continued)*

Star	Δα (arcsec)	Δδ (arcsec)	V (mag)	(B-V) (mag)	N_*	N_b	Other Identifications
36	-30.3	1266.0	15.70	0.63	4	4	
37	-33.4	1248.3	13.32	0.39	4	4	AR162
			Region 4				
1	591.8	-320.8	15.22	0.39	1	1	
2	591.2	-390.8	13.19	0.11	1	1	
3	585.5	-476.3	15.50	0.57	1	1	
4	578.6	-398.0	14.90	1.60	1	1	
5	571.1	-512.8	11.31	0.05	1	1	
6	558.6	-504.4	14.86	1.40	1	1	
7	539.4	-503.1	13.24	0.96	1	1	
8	534.9	-364.4	15.90	0.62	1	1	
9	503.0	-466.6	15.35	0.53	1	1	
10	489.7	-321.2	13.23	0.27	1	1	
11	480.0	-325.0	14.89	0.52	1	1	
12	449.4	-322.5	13.77	1.03	1	1	
13	447.1	-398.7	15.15	1.56	1	1	
14	425.5	-366.5	14.97	0.44	1	1	
15	424.1	-325.3	11.04	1.40	1	1	
16	401.1	-408.2	12.52	0.20	1	1	
17	393.6	-455.2	14.17	1.08	1	1	AR197
18	377.3	-399.7	14.63	0.53	1	1	
19	312.4	-405.0	14.64	1.42	1	1	
20	309.5	-427.2	15.72	1.05	1	1	
21	307.1	-330.2	15.05	0.81	1	1	
22	304.3	-327.5	15.57	1.01	1	1	
23	303.6	-319.5	14.91	1.36	1	1	
24	282.9	-319.8	14.00	0.14	1	1	
25	279.5	-453.3	14.59	0.19	1	1	AR191
26	274.3	-336.9	16.00	0.59	1	1	
27	266.8	-371.0	14.25	1.48	1	1	
28	234.3	-488.8	15.31	1.14	1	1	
29	219.5	-382.9	14.14	1.23	1	1	
30	217.3	-515.1	14.90	0.56	1	1	
31	211.8	-466.4	14.42	1.07	1	1	AR185
32	198.1	-438.4	15.36	0.45	1	1	
33	192.0	-503.8	15.91	0.65	1	1	
34	173.3	-487.3	15.64	0.64	1	1	
35	172.3	-465.5	15.75	1.06	1	1	
36	171.3	-408.0	13.44	0.30	1	1	AR182
37	168.8	-524.0	15.45	0.50	1	1	
38	156.3	-367.7	15.79	0.67	1	1	
39	155.4	-461.4	14.88	0.92	1	1	
40	146.4	-394.4	14.25	0.61	1	1	
41	139.8	-355.7	10.50	-0.01	1	1	
42	124.2	-506.5	15.31	0.53	1	1	
43	124.5	-332.7	10.85	0.06	1	1	
44	90.9	-516.6	15.36	0.65	1	1	
45	75.8	-377.9	15.37	0.57	1	1	
46	71.1	-380.5	15.79	0.60	1	1	
47	65.5	-376.3	15.76	0.65	1	1	
48	55.9	-339.1	12.00	0.19	1	1	
49	35.0	-524.5	15.80	0.56	1	1	
50	33.9	-467.0	13.92	1.45	1	1	
51	33.5	-402.7	14.95	0.30	1	1	
			Region 5				
1	906.0	-259.5	15.66	0.69	1	1	
2	901.4	-190.9	15.93	0.29	1	1	
3	895.3	-254.9	15.75	0.33	1	1	
4	889.9	-216.4	14.45	0.44	1	1	
5	851.6	-253.1	14.07	1.26	1	1	
6	841.1	-182.4	13.79	0.29	1	1	
7	838.6	-299.9	14.98	1.18	1	1	
8	837.4	-143.8	14.85	0.53	1	1	
9	824.0	-187.1	14.69	0.21	1	1	
10	808.7	-167.5	14.76	0.55	1	1	
11	807.7	-233.5	15.97	0.52	1	1	
12	790.0	-305.7	15.85	0.35	1	1	
13	784.9	-193.9	14.56	0.51	1	1	
14	780.4	-299.9	14.27	1.08	1	1	
15	767.9	-136.4	13.76	1.72	1	1	
16	764.2	-127.0	13.43	1.82	1	1	
17	750.6	-291.8	14.67	1.44	1	1	
18	745.0	-103.6	12.01	0.26	1	1	
19	734.0	-236.8	13.04	1.61	1	1	
20	688.0	-121.2	15.69	0.84	1	1	
21	643.5	-239.2	14.49	0.49	1	1	AR214
22	642.9	-268.3	13.18	0.27	1	1	AR212
23	641.7	-216.7	14.90	1.06	1	1	
24	637.6	-120.4	15.78	0.83	1	1	
25	619.7	-208.5	15.09	0.91	1	1	
26	613.4	-253.4	14.34	1.09	1	1	AR208
27	612.0	-141.6	14.45	0.63	1	1	
28	583.4	-184.3	14.47	0.64	1	1	
29	582.9	-146.9	15.96	0.74	1	1	
30	558.6	-271.7	15.53	0.62	1	1	
31	550.6	-139.7	15.98	0.50	1	1	
32	523.6	-214.4	14.28	1.82	1	1	
33	521.7	-183.5	13.63	0.46	1	1	
34	510.2	-271.8	15.90	0.82	1	1	
35	505.8	-204.3	15.43	0.70	1	1	
36	487.8	-113.6	13.98	1.43	1	1	
37	474.4	-245.0	15.82	0.69	1	1	
38	461.8	-306.7	13.95	0.86	1	1	
39	450.9	-304.6	14.96	0.61	1	1	
40	448.0	-226.3	15.82	0.74	1	1	
41	444.6	-170.9	14.03	0.74	1	1	
42	443.3	-297.7	14.76	0.65	1	1	
43	435.6	-142.6	15.30	0.72	1	1	
44	433.9	-207.5	14.68	1.36	1	1	
45	427.9	-232.3	15.07	0.47	1	1	
46	413.7	-138.2	14.41	1.15	1	1	
47	406.8	-273.2	13.50	0.43	1	1	
48	379.0	-265.5	12.96	1.21	1	1	
49	379.2	-115.7	13.22	0.46	1	1	
50	370.8	-192.4	15.97	0.83	1	1	
51	363.2	-260.5	15.25	0.32	1	1	
52	362.8	-301.9	15.36	1.33	1	1	
53	340.2	-238.2	15.94	0.54	1	1	
54	287.2	-151.6	14.63	1.45	1	1	
			Region 6				
1	1248.8	-393.1	14.53	0.53	1	1	
2	1230.2	-468.9	13.97	0.81	1	1	
3	1206.7	-331.0	14.75	0.57	1	1	
4	1197.2	-350.4	16.00	0.54	1	1	
5	1195.4	-491.0	15.79	0.49	1	1	
6	1190.9	-453.3	15.58	1.09	1	1	
7	1173.0	-385.0	14.62	1.11	1	1	
8	1167.8	-505.0	14.36	1.01	1	1	
9	1147.6	-389.0	12.41	1.00	1	1	
10	1143.7	-517.4	12.16	1.21	1	1	AR235
11	1134.4	-376.9	15.13	1.03	1	1	
12	1125.7	-501.1	15.86	1.11	1	1	
13	1117.6	-337.4	15.42	1.32	1	1	
14	1103.6	-434.1	14.80	1.56	1	1	
15	1102.0	-434.8	13.27	0.82	1	1	
16	1062.5	-447.2	11.76	0.57	1	1	
17	1051.0	-344.9	15.15	0.49	1	1	
18	1049.6	-388.4	15.88	0.38	1	1	
19	1036.2	-458.6	15.82	0.57	1	1	
20	1032.9	-515.5	13.56	0.48	1	1	AR233
21	1002.8	-401.0	15.75	0.49	1	1	
22	993.0	-434.7	15.14	0.54	1	1	
23	985.9	-454.9	13.10	0.63	1	1	AR230
24	977.7	-504.2	12.75	1.03	1	1	AR229
25	970.0	-347.4	13.66	0.45	1	1	
26	966.0	-473.6	15.54	1.15	1	1	
27	964.4	-379.6	14.52	1.09	1	1	
28	957.0	-488.5	14.83	1.23	1	1	

TABLE 2. *(continued)*

Star	Δα (arcsec)	Δδ (arcsec)	V (mag)	(B-V) (mag)	N_v	N_b	Other Identifications
29	955.4	-320.7	13.89	0.35	1	1	
30	927.8	-451.8	15.03	0.62	1	1	
31	907.1	-441.8	15.68	0.53	1	1	
32	905.9	-482.0	14.50	0.56	1	1	
33	878.9	-396.1	12.95	1.52	1	1	
34	877.8	-463.2	14.94	1.57	1	1	
35	870.0	-327.1	14.30	0.49	1	1	
36	847.8	-423.3	12.26	0.08	1	1	
37	837.9	-335.2	14.98	0.46	1	1	
38	819.2	-410.8	15.41	0.45	1	1	
39	765.7	-485.5	15.72	0.42	1	1	
40	758.0	-440.8	15.37	0.46	1	1	
41	748.5	-424.4	12.90	0.91	1	1	AR218
42	738.8	-400.5	14.87	1.33	1	1	
43	730.4	-326.8	15.20	0.39	1	1	
44	719.3	-397.3	15.75	0.51	1	1	
45	713.8	-411.0	14.08	1.80	1	1	
46	695.7	-518.3	15.54	0.56	1	1	
47	672.7	-376.5	13.19	0.32	1	1	AR215
48	661.9	-434.7	15.68	1.29	2	2	
49	627.5	-518.3	14.94	0.33	2	2	
50	627.0	-324.7	14.38	0.44	2	2	
51	622.1	-433.3	15.53	1.26	2	2	
			Region 7				
1	1805.7	41.5	15.76	0.60	3	2	
2	1782.2	-82.8	14.19	1.31	3	3	
3	1769.3	28.6	15.97	0.68	3	3	
4	1759.1	-26.8	14.46	1.07	3	3	
5	1748.6	17.1	14.39	1.23	3	3	
6	1744.8	66.6	15.36	1.18	3	3	
7	1724.8	38.5	11.78	0.36	3	3	JM212,L26
8	1714.7	65.1	14.83	0.72	3	3	
9	1705.0	-120.4	15.41	0.88	3	3	
10	1703.4	-9.9	15.18	1.70	3	3	
11	1696.1	-80.1	12.66	0.66	3	3	
12	1689.1	-90.4	15.87	0.62	3	3	
13	1679.3	-124.0	15.24	0.59	3	3	
14	1676.8	-114.5	15.82	0.42	3	3	
15	1666.9	40.5	13.67	0.56	3	3	
16	1666.5	-99.3	15.16	0.68	3	3	
17	1666.9	74.3	14.46	0.36	3	3	
18	1639.2	78.5	15.57	0.46	3	3	
19	1631.6	23.6	14.20	0.39	3	3	
20	1629.7	-43.2	13.53	0.14	3	3	
21	1615.7	-106.8	15.40	0.47	3	3	
22	1608.0	-59.4	15.18	0.59	3	3	
23	1606.5	66.1	15.50	0.79	3	3	
24	1605.2	-5.2	15.16	1.11	3	2	
25	1591.1	31.6	15.67	0.63	3	3	
26	1588.0	-49.7	15.51	0.62	3	3	
27	1584.2	-95.1	14.24	0.64	3	3	
28	1577.1	-115.1	15.45	1.19	3	2	
29	1556.9	53.0	14.11	0.52	3	3	
30	1548.6	-114.0	15.28	1.22	3	3	
31	1537.9	-116.1	14.91	0.89	3	3	
32	1531.7	-18.5	14.26	0.53	3	3	
33	1513.2	46.3	14.67	0.64	3	3	
34	1506.4	22.7	16.00	0.90	3	2	
35	1498.9	36.4	15.31	1.21	3	3	
36	1488.8	17.6	14.63	0.28	3	3	
37	1449.7	-21.9	13.38	0.44	3	3	AR251
38	1449.2	5.8	14.98	1.81	3	3	
39	1443.4	65.1	14.45	0.59	3	3	
40	1431.6	55.5	15.94	0.80	3	3	
41	1405.0	24.1	15.13	0.79	3	3	
42	1403.1	13.7	15.15	0.60	3	3	
43	1395.8	43.1	15.67	0.62	3	3	
44	1392.5	-11.4	15.13	1.31	3	3	
45	1386.8	-46.3	14.33	1.53	3	3	
46	1374.8	2.2	15.40	1.37	3	3	
47	1360.9	-5.0	14.74	1.12	3	3	
48	1354.9	37.5	9.82	0.05	3	3	JM211,L18
49	1340.3	-65.9	13.05	1.52	3	3	AR246
50	1336.2	51.0	15.25	0.82	3	3	
51	1313.6	65.6	13.79	0.39	3	3	
52	1291.8	27.9	14.39	0.69	3	3	
53	1291.2	-91.2	13.39	0.53	3	3	
54	1291.4	60.5	15.40	1.40	3	3	
55	1268.9	-123.9	15.80	0.79	3	3	
56	1253.1	-66.2	15.18	1.13	3	3	
57	1252.7	48.5	12.58	1.42	3	3	AR242
58	1241.6	-7.9	15.25	0.80	3	3	
59	1238.0	-124.2	13.18	1.20	3	3	
60	1205.3	6.9	13.74	0.83	3	3	
61	1202.5	53.6	14.41	0.39	3	3	AR237
62	1196.4	-14.3	15.35	0.48	3	3	

TABLE 3. *Comparison of photographic B magnitudes and spectroscopic (B-V) colours with independent photometry. A reddening correction of E(B-V)=0.04 mag has been applied. Differences (Δ) are always in the sense of independent data minus value given in Table 4. N denotes the number of common stars.*

ΔB		Δ(B-V)		N	Source
Mean	σ	Mean	σ		
0.08	0.13	-0.02	0.07	5	Jankowitz & McCosh (1963)
-0.07	0.12	0.00	0.12	12	Present CCD data

TABLE 4. *Photographic B magnitude, (B-V) colour, MK spectral type, heliocentric velocity and internal error, apparent distance modulus and membership status for the stars observed spectroscopically. Star identifications in col. 1 are taken from Andersen and Reiz (1983).*

Star	B	$(B-V)_0$	Sp. type	Hel. Vel.	±	Error	$m-M_v$	Membership	Remarks
17	13.24	0.18	A6 V	7.5	±	15	10.92	M	
22	13.10	0.64	G0 III	13.2	±	15	11.42	NM	
27	13.72	0.95	G7 III	-29.3	±	12	11.88	NM	
29	13.64	0.49	F6 V	35.0	±	10	9.31	NM	
34	13.91	0.49	F4 III	36.6	±	9	11.73	NM	
35	13.56	0.26	F0 III	-11.4	±	12	11.76	NM	
38	13.94	0.34	A8 V	-0.8	±	14	11.16	M	
46	13.97	0.64	G0 III	-6.8	±	15	12.29	NM	
47	14.78	0.49	F4 III	-24.3	±	11	12.60	NM	
48	14.64	0.64	G2 IV	63.2	±	20	10.96	NM	
52	15.83	0.44	F6 III	45.2	±	18	13.85	NM	
63	14.13	1.17	K2 III	-28.6	±	8	12.42	NM	
64	14.49	0.49	F4 III	69.8	±	11	12.31	NM	
72	13.88	0.20	A7 V	-5.1	±	12	11.44	M	
73	13.52	0.34	A8 V	0.5	±	15	10.74	M	JM39
77	14.42	0.26	F0 III	-11.6	±	11	12.62	NM	
78	15.26	0.60	F8 V	-9.4	±	22	10.62	M	
82	14.74	0.44	F6 III	-14.9	±	8	12.76	NM	
85	15.18	0.49	F4 III	18.1	±	11	13.00	NM	
88	14.92	0.49	F4 III	-65.6	±	15	12.77	NM	
92	14.04	0.30	A9 V	2.1	±	10	11.20	M	R1,CCD
93	15.37	0.44	F6 III	16.1	±	17	13.39	NM	
94	13.40	0.20	A7 V	-13.5	±	12	10.96	M	JM69
95	14.05	0.34	A8 V	9.5	±	13	11.27	M	R1,CCD
99	14.61	0.80	G9 V	-12.6	±	12	8.07	NM	
121	15.57	0.34	A8 V	-19.0	±	17	12.79	NM	
129	15.02	0.44	F6 III	17.0	±	11	13.04	NM	
138	14.22	0.47	F5 V	18.0	±	11	10.21	M	JM134
139	15.71	0.44	F6 III	-22.7	±	12	13.73	NM	
144	14.72	0.34	A8 V	0.5	±	14	11.94	NM	R2,CCD
148	14.34	1.24	K5 V	3.4	±	14	5.71	NM	JM152
151	14.61	0.26	F0 III	32.1	±	10	12.81	NM	
152	14.70	0.49	F4 III	3.8	±	10	12.52	NM	
154	14.76	0.44	F6 III	2.3	±	11	12.78	NM	
167	14.46	1.24	K5 V	45.0	±	17	5.83	NM	R3,CCD
170	14.81	0.34	A8 V	-15.4	±	15	11.99	NM	
173	13.49	0.20	A7 V	12.6	±	9	11.05	M	JM172
185	15.68	1.24	K5 V	21.6	±	9	7.05	NM	R4,CCD
189	14.34	1.45	K4 III	20.0	±	12	12.85	NM	
194	14.16	0.64	G2 IV	71.9	±	13	10.48	NM	R3,CCD
197	15.26	1.17	K2 III	-22.5	±	10	13.55	NM	R4,CCD
200	14.39	0.30	A9 V	13.5	±	11	11.50	M	
204	13.87	0.42	F3 V	-13.6	±	9	9.83	M	
213	14.89	0.44	F6 III	10.2	±	15	12.91	NM	
214	14.83	0.26	F0 III	27.3	±	9	13.03	NM	R5,CCD
216	14.82	0.64	G0 III	13.7	±	11	13.14	NM	
217	13.59	0.44	F6 III	23.1	±	16	11.61	NM	
218	13.98	0.95	G7 III	-32.3	±	13	12.14	NM	R6,CCD
222	14.96	0.34	A8 V	54.7	±	12	12.18	NM	
228	15.25	0.33	F0 V	-2.8	±	12	12.18	NM	
230	13.76	0.64	G0 III	27.7	±	18	12.08	NM	R6,CCD
232	14.32	0.44	F6 III	6.7	±	14	12.34	NM	
246	14.66	1.32	K3 III	15.4	±	10	13.00	NM	R7,CCD
251	13.83	0.34	A8 V	1.1	±	10	11.06	M	R7,CCD
254	14.38	0.20	A7 V	4.2	±	11	11.94	NM	

TABLE 5. *Line indices and continuum ratios for stars observed spectroscopically. Star numbering is the same as in Table 4. Stars showing emission in the CaII H and K line cores have been identified in the last column.*

Star	3912/3990	H	K	Ca	HK	Remarks
17	0.671±0.020	0.520±0.013	0.302±0.009	0.822±0.016	0.117±0.005	Ca II emitter
22	0.589±0.007	0.286±0.004	0.344±0.004	0.630±0.005	0.073±0.002	
27	0.502±0.009	0.219±0.004	0.296±0.005	0.515±0.007	0.061±0.002	
29	0.657±0.009	0.324±0.004	0.353±0.004	0.677±0.006	0.074±0.002	
34	0.672±0.016	0.378±0.008	0.367±0.008	0.746±0.012	0.076±0.003	
35	0.651±0.009	0.391±0.005	0.341±0.004	0.732±0.007	0.075±0.002	
38	0.664±0.014	0.419±0.008	0.355±0.007	0.774±0.011	0.084±0.003	
46	0.583±0.010	0.270±0.005	0.353±0.006	0.623±0.008	0.071±0.003	
47	0.618±0.020	0.324±0.010	0.375±0.011	0.698±0.015	0.083±0.005	
48	0.533±0.018	0.275±0.010	0.333±0.011	0.608±0.014	0.073±0.005	
52	0.557±0.029	0.353±0.017	0.403±0.018	0.756±0.025	0.095±0.008	
63	0.378±0.034	0.123±0.015	0.291±0.025	0.414±0.029	0.049±0.012	
64	0.621±0.010	0.303±0.005	0.364±0.006	0.666±0.008	0.078±0.003	
72	0.683±0.006	0.403±0.004	0.372±0.003	0.775±0.005	0.081±0.001	
73	0.697±0.007	0.456±0.004	0.325±0.003	0.781±0.005	0.087±0.002	
77	0.668±0.009	0.372±0.005	0.376±0.005	0.748±0.007	0.083±0.002	
78	0.579±0.018	0.322±0.010	0.388±0.011	0.710±0.015	0.112±0.006	Ca II emitter
82	0.643±0.011	0.343±0.005	0.377±0.006	0.720±0.008	0.086±0.003	
85	0.631±0.013	0.334±0.007	0.369±0.007	0.703±0.010	0.083±0.003	
88	0.597±0.037	0.345±0.020	0.340±0.020	0.685±0.029	0.083±0.009	
92	0.664±0.008	0.397±0.004	0.384±0.004	0.782±0.006	0.082±0.002	
93	0.639±0.014	0.320±0.007	0.373±0.008	0.693±0.010	0.093±0.004	
94	0.612±0.011	0.404±0.007	0.344±0.006	0.747±0.009	0.075±0.003	
95	0.706±0.010	0.478±0.006	0.407±0.005	0.885±0.008	0.122±0.003	Ca II emitter
99	0.560±0.015	0.288±0.008	0.315±0.008	0.603±0.011	0.097±0.005	
121	0.671±0.029	0.524±0.019	0.302±0.013	0.826±0.023	0.111±0.007	Ca II emitter
129	0.654±0.020	0.308±0.010	0.339±0.010	0.647±0.014	0.081±0.005	
138	0.581±0.015	0.355±0.009	0.361±0.009	0.716±0.013	0.080±0.004	
139	0.680±0.020	0.315±0.009	0.358±0.010	0.673±0.014	0.078±0.005	
144	0.701±0.010	0.498±0.006	0.306±0.004	0.804±0.007	0.111±0.002	Ca II emitter
148	0.489±0.015	0.242±0.008	0.313±0.009	0.555±0.012	0.070±0.005	
151	0.640±0.011	0.403±0.006	0.334±0.005	0.737±0.008	0.079±0.002	
152	0.621±0.011	0.352±0.006	0.375±0.006	0.727±0.008	0.098±0.003	
154	0.667±0.035	0.334±0.017	0.332±0.017	0.665±0.024	0.072±0.008	
167	0.437±0.040	0.191±0.020	0.276±0.025	0.468±0.032	0.047±0.011	
170	0.703±0.011	0.462±0.007	0.294±0.005	0.756±0.008	0.087±0.003	
173	0.650±0.007	0.407±0.004	0.371±0.004	0.778±0.006	0.081±0.002	
185	0.467±0.016	0.193±0.007	0.297±0.010	0.490±0.012	0.070±0.005	
189	0.437±0.032	0.194±0.016	0.274±0.020	0.468±0.025	0.030±0.007	
194	0.552±0.031	0.221±0.014	0.300±0.017	0.521±0.022	0.049±0.007	
197	0.463±0.016	0.213±0.008	0.291±0.010	0.504±0.013	0.071±0.005	
200	0.674±0.016	0.402±0.009	0.333±0.008	0.735±0.011	0.066±0.003	
204	0.652±0.007	0.348±0.004	0.365±0.004	0.712±0.005	0.075±0.002	
213	0.760±0.038	0.329±0.016	0.356±0.017	0.686±0.024	0.065±0.007	
214	0.675±0.012	0.401±0.006	0.377±0.006	0.778±0.009	0.067±0.002	
216	0.618±0.013	0.283±0.006	0.343±0.007	0.626±0.009	0.071±0.003	
217	0.641±0.030	0.367±0.016	0.350±0.015	0.717±0.022	0.065±0.006	
218	0.493±0.008	0.234±0.004	0.310±0.005	0.544±0.006	0.065±0.002	
222	0.713±0.029	0.532±0.018	0.255±0.011	0.787±0.021	0.131±0.008	Ca II emitter
228	0.592±0.027	0.333±0.015	0.365±0.016	0.699±0.022	0.080±0.007	
230	0.551±0.008	0.260±0.004	0.336±0.004	0.596±0.006	0.070±0.002	
232	0.656±0.023	0.326±0.011	0.366±0.012	0.692±0.017	0.067±0.005	
246	0.360±0.023	0.166±0.012	0.341±0.019	0.507±0.023	0.053±0.008	
251	0.654±0.011	0.425±0.007	0.365±0.006	0.790±0.009	0.086±0.003	
254	0.708±0.025	0.386±0.013	0.368±0.012	0.754±0.018	0.069±0.005	

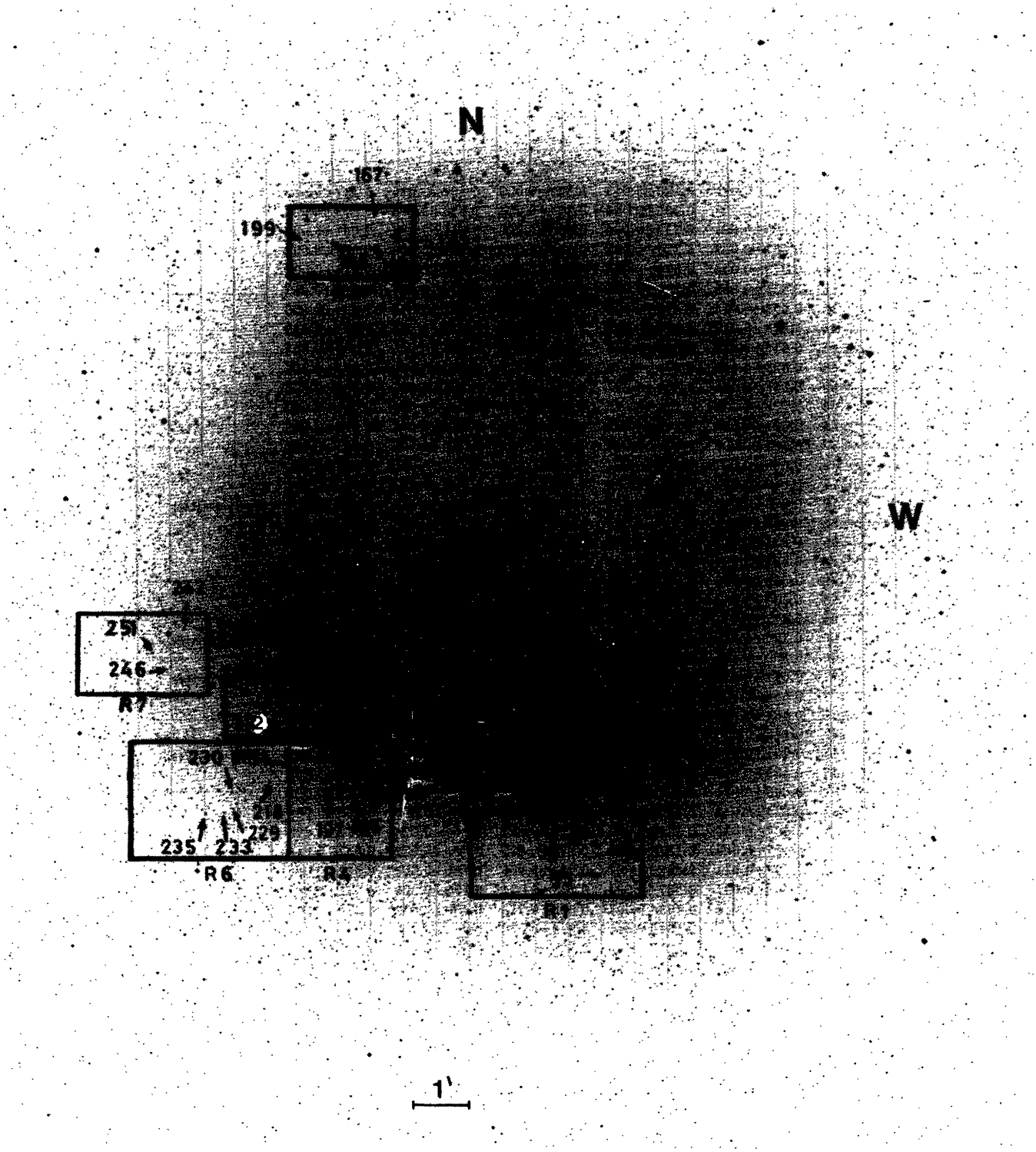

FIGURE 1. Identification chart for the regions R1-R7 imaged using the CCD camera. The reproduction is from a 5 minute exposure AAT prime focus photographic plate taken using IIaO emulsion and a GG385 filter. THe identification numbers denote the stars with astrometric measurements by Andersen and Reiz (1983).

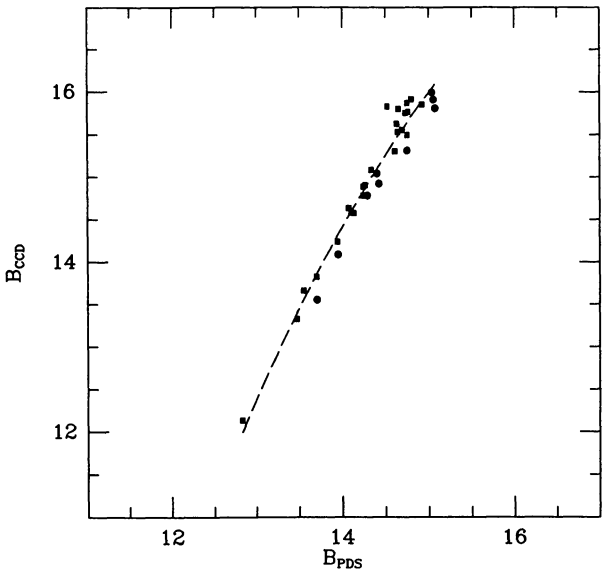

FIGURE 2. Calibration curve used to convert the PDS photographic B magnitudes onto the CCD system. Filled circles denote the comparison in region R3 (cf. Fig. 1), squares are for stars in R7. The rms residual about the fitted relation (dashed line) is 0.18 mag.

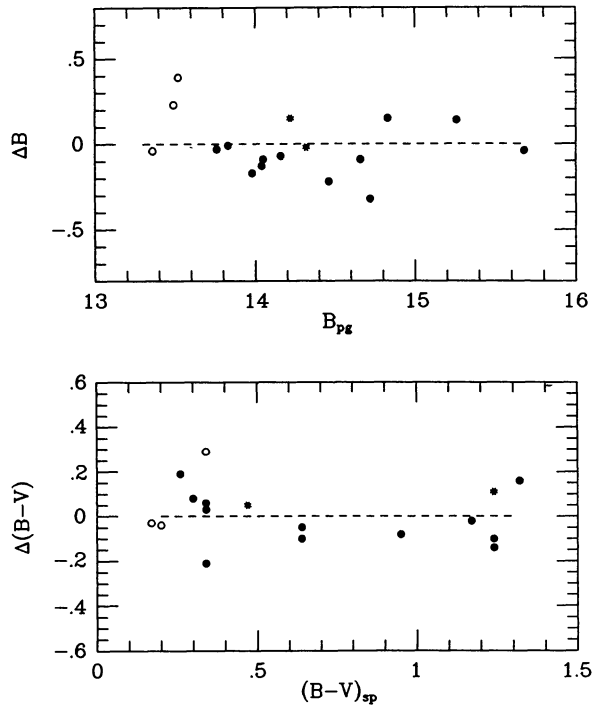

FIGURE 3. Comparison of the transformed photographic magnitudes B_{pg} and spectroscopic $(B-V)_{sp}$ colours with photographic (o) and photoelectric (*) photometry from Jankowitz and McCosh (1963) and the present CCD observations (•). The difference Δ is in the sense of independent data minus B_{pg} or $(B-V)_{sp}$.

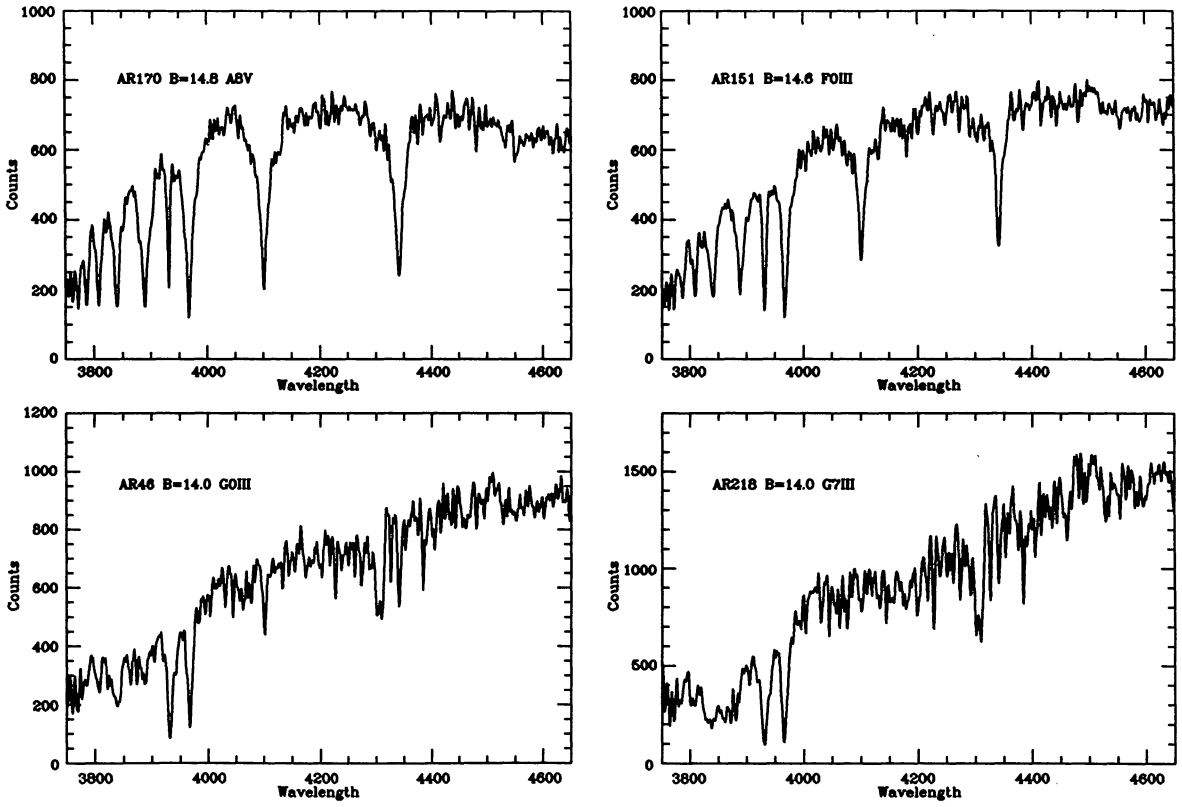

FIGURE 4. Example spectra showing the range of feature strengths in the spectroscopic sample. The spectral types are determined *via* a cross-correlation technique as discussed in the text.

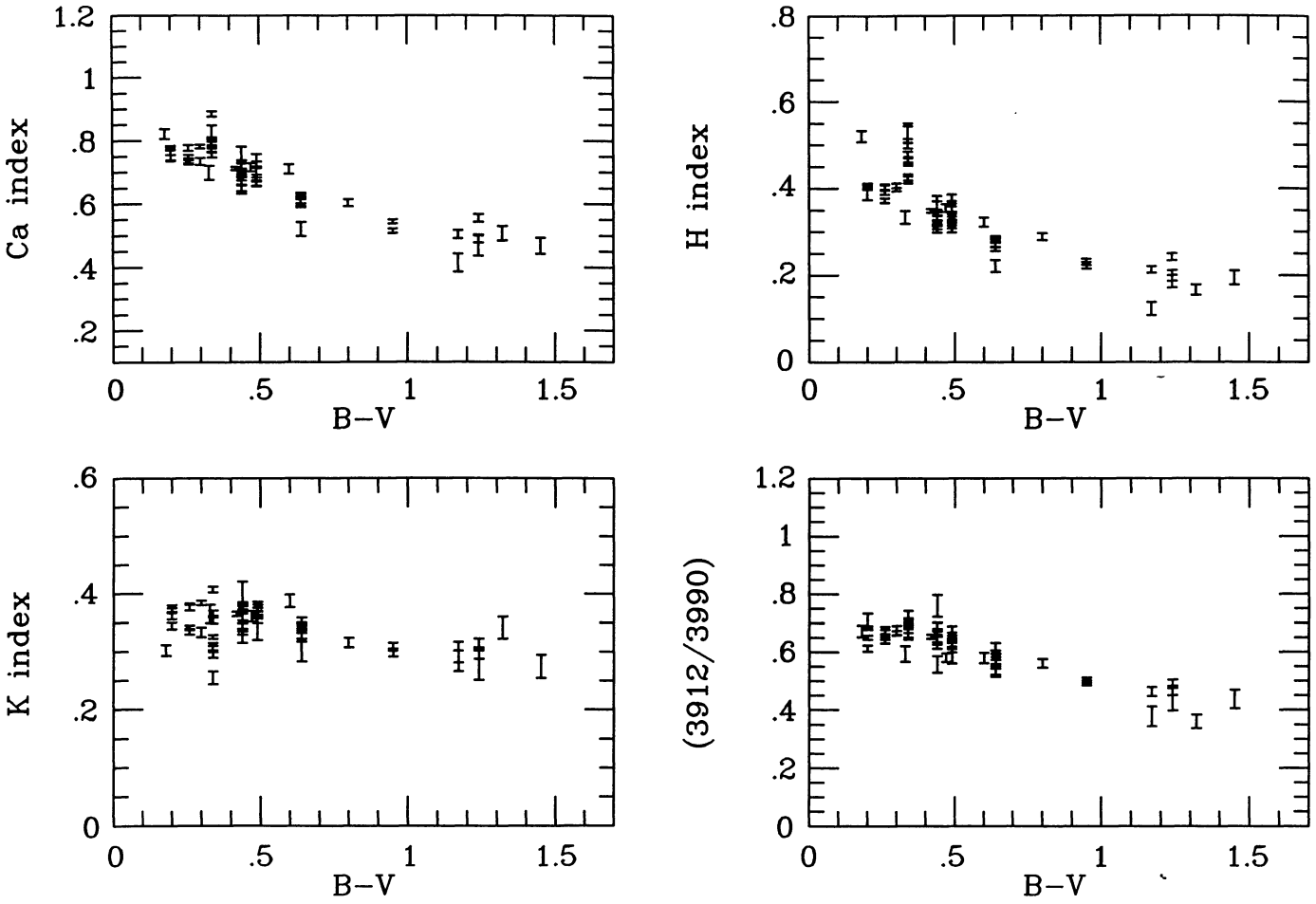

FIGURE 5. Plot of spectroscopic line indices against $(B - V)$ colour. Since the line indices are sensitive to sky-subtraction and flux-calibration errors, the good correlations seen in this figure confirm the quality of the spectroscopic data.

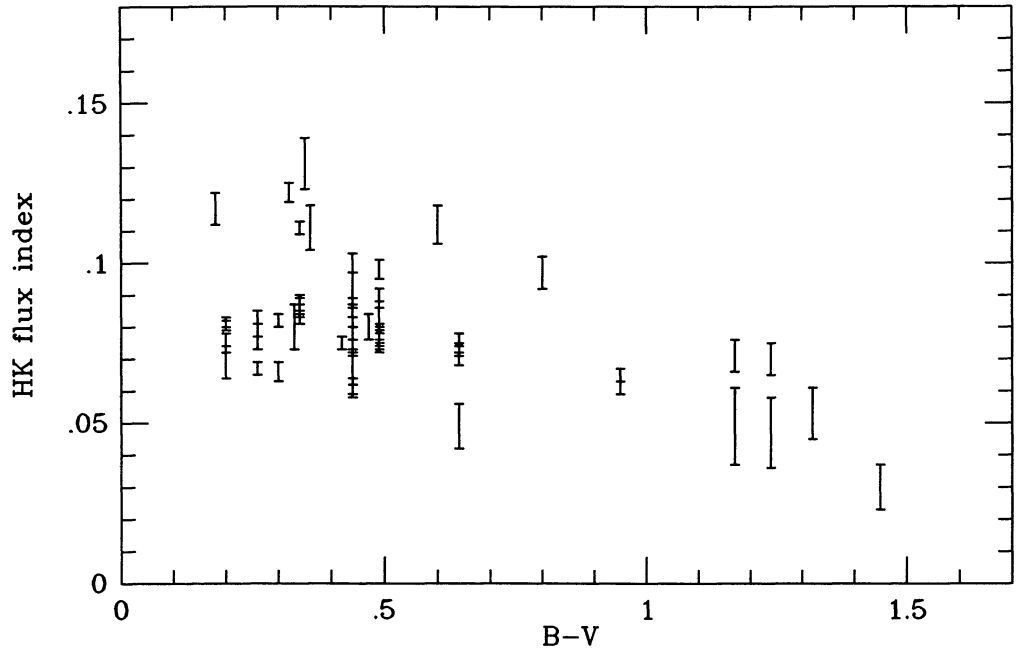

FIGURE 6. HK flux index *versus* $(B - V)$ colour. Error bars are derived from the photon counts in each spectrum asuming Poisson statistics. The 6 stars with $HK > 0.1$ are probably chromospherically active stars in which emission line cores in the CaII lines have increased the HK flux ratio.

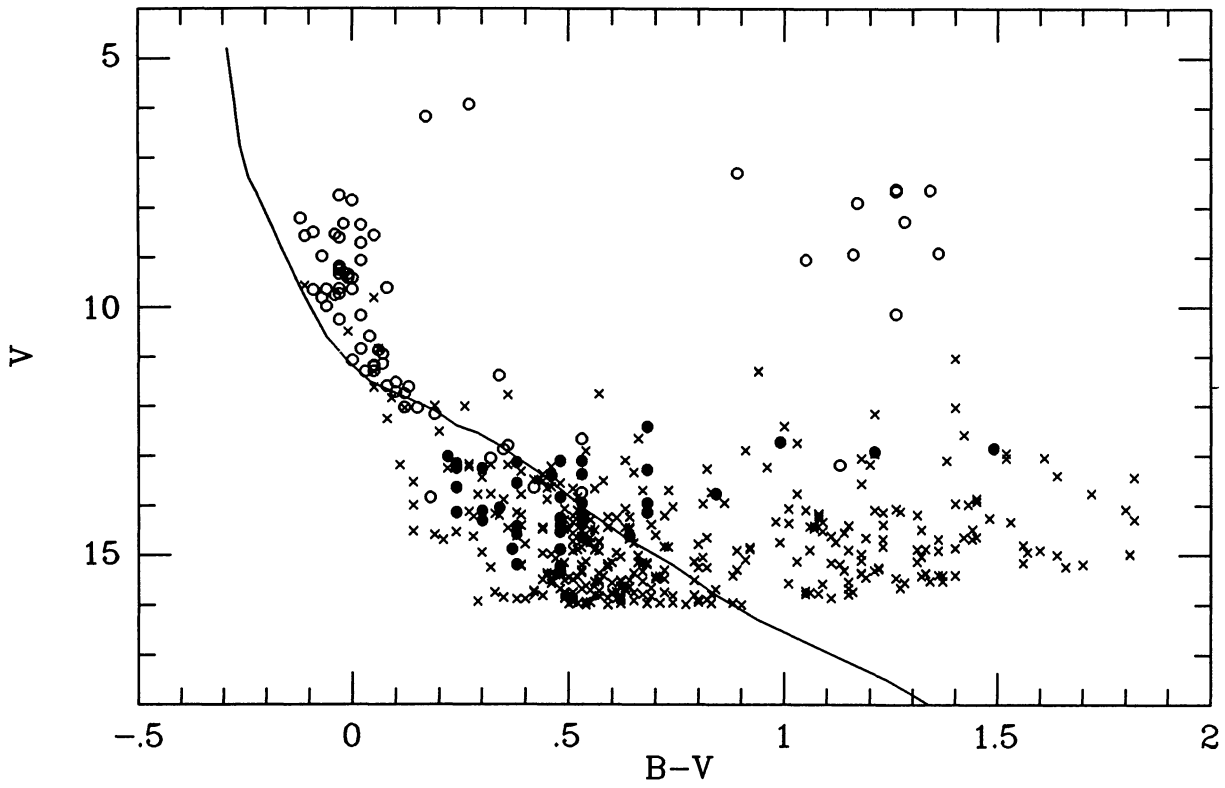

FIGURE 7. A $(V, B-V)$ colour-magnitude diagram for NGC 3114 based on photoelectric observations (o) from the literature and CCD observations from Table 2 (×). The stars in the spectroscopic sample which have B magnitudes determined *via* photographic photometry and $B-V$ colours from spectral classification are shown using the • symbol. The solid line shows the fitted ZAMS (see text).

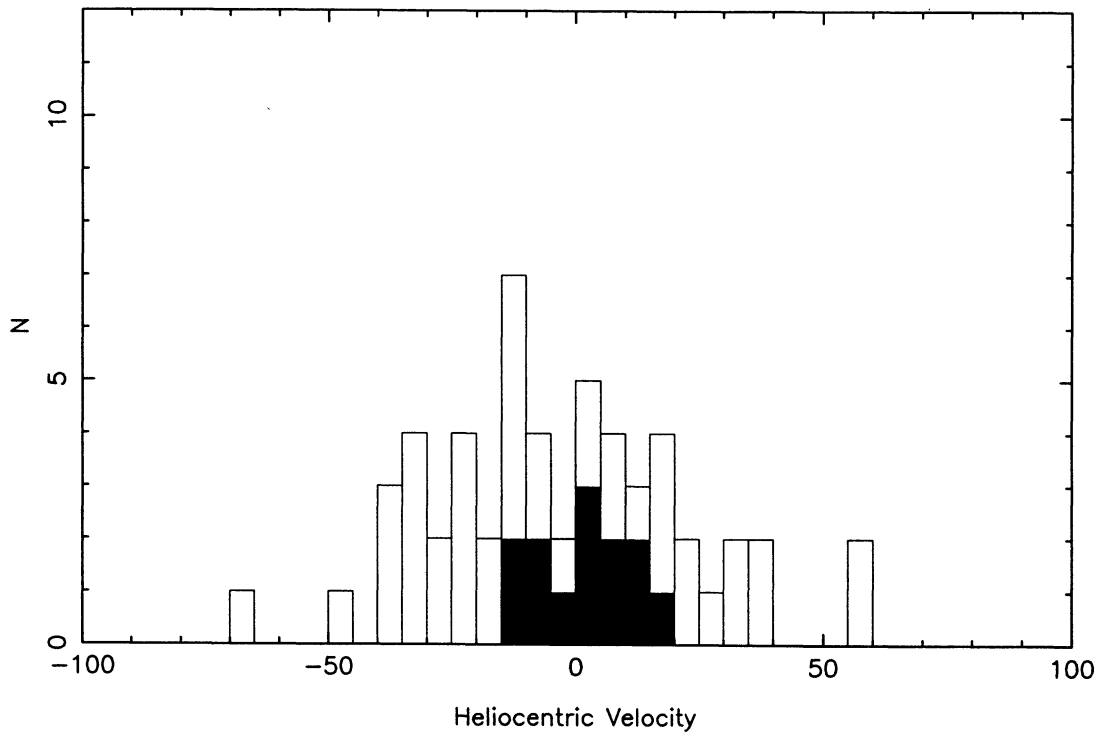

FIGURE 8. Histogram of radial velocities of the spectroscopic stars. Filled area shows only those stars classified as cluster members in Table 4.

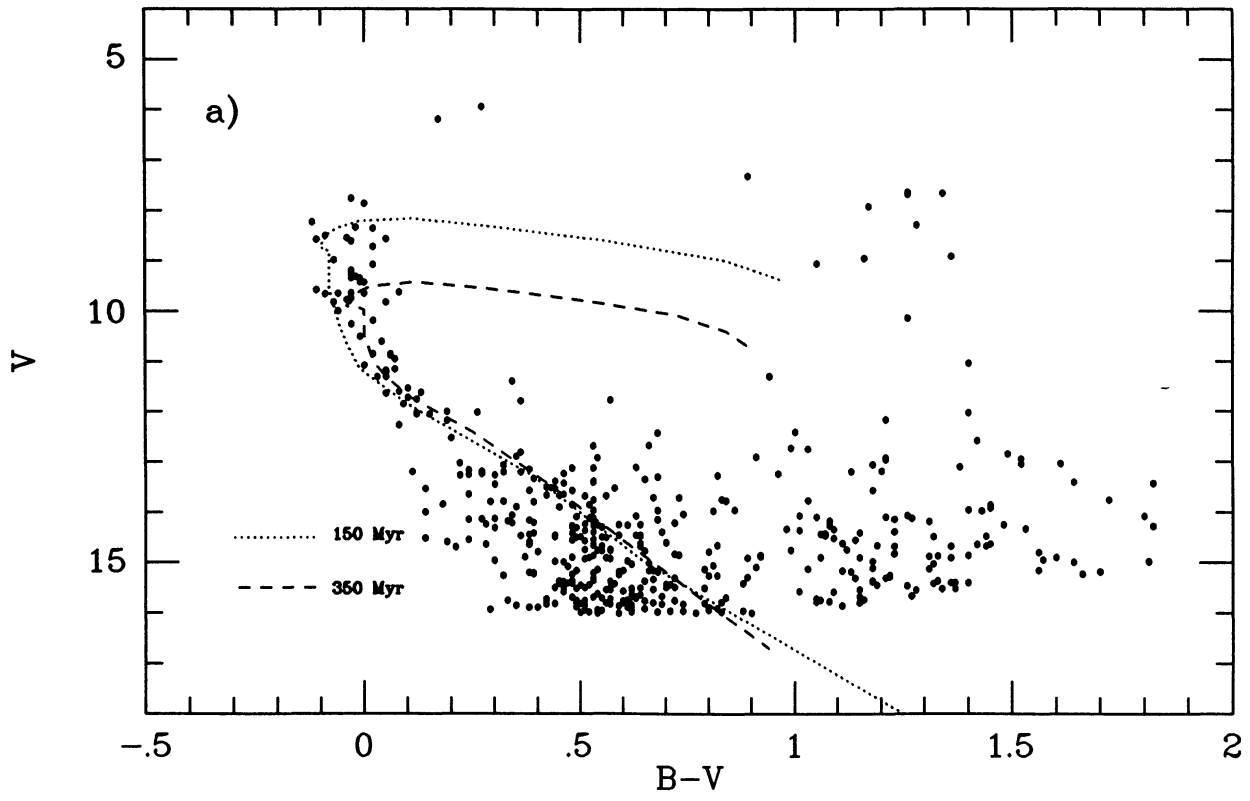

FIGURE 9a.

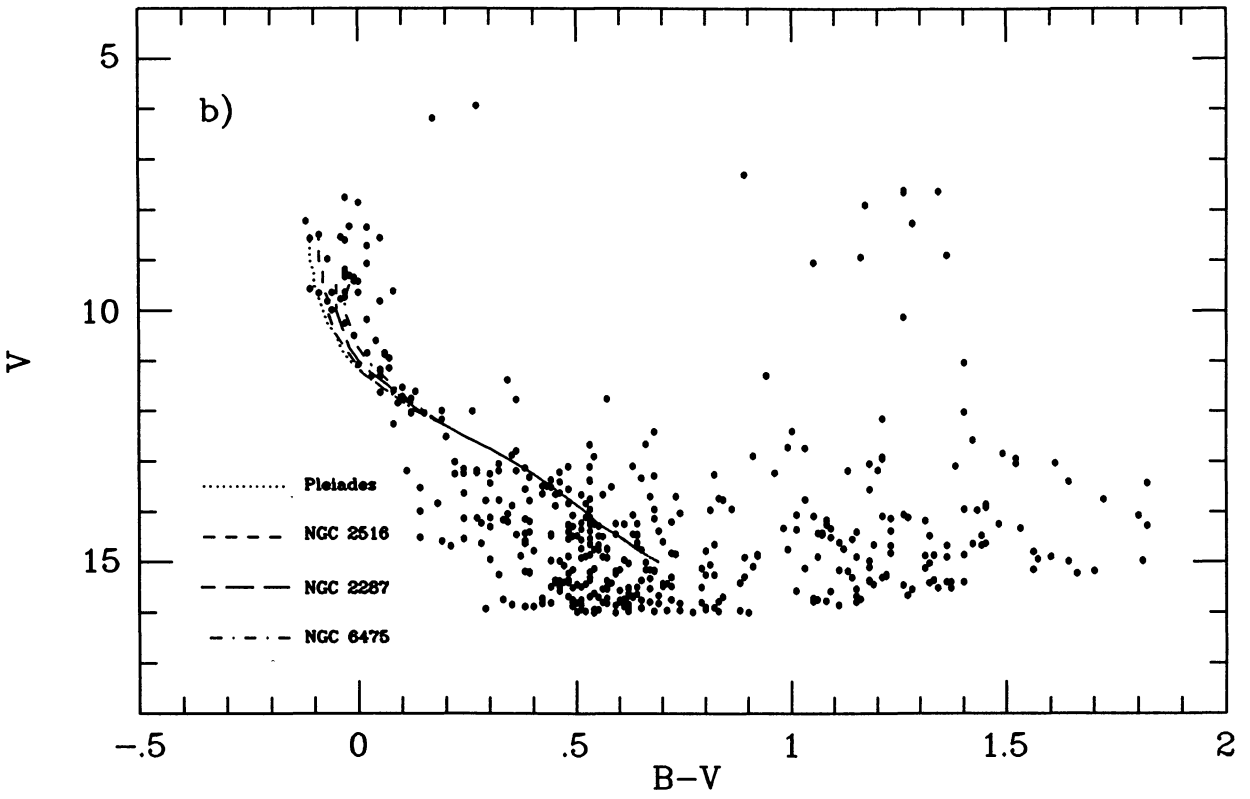

FIGURE 9b.

FIGURE 9. Isochrone fits to the CMD of NGC 3114: a) Theoretical tracks for $Z = 0.01$ and $Y = 0.20$; b) Empirical isochrones for the Pleiades, NGC 2516, NGC 2287 and NGC 6475 age groups.